Magnetic Materials Enriched with Strontium: a Study of the use as Catalysts in the Transesterification Reaction of Babassu Oil

Wiury Chaves de Abreu[a,b] [ID]*, Ana Flávia Moraes[a], Roberta Yonara Nascimento Reis[a], Bernardo Ferreira*

Pinto[a] [ID]*, Carla Verônica Rodarte de Moura[a]* [ID]*, Sabrina Nicolodi[c], Edmilson Miranda de Moura[a]** [ID]

[a]Departamento de Química, Universidade Federal do Piauí, Teresina, PI, Brasil
[b]Instituto Federal de Educação, Ciência e Tecnologia do Maranhão, Buriticupu, MA, Brasil
[c]Instituto de Física, Universidade Federal do Rio Grande do Sul, Porto Alegre, RS, Brasil

This work described a new magnetic material enriched with strontium as catalyst to produce babassu biodiesel. The use of magnetic materials has attracted attention due to easy and fast separation from reaction medium. Moreover, they are ecologically correct, due to they generate less discards to the environment. Techniques of analysis and characterization were carried out to check the synthesis of magnetite and strontium ferrite, besides to verify the presence of hydroxide and carbonate in the structure of the strontium oxide. The best catalytic activities presented conversions of 78.6% and 89.7% when using the catalysts SrO/Fe_3O_4 and $SrO/SrFe_2O_4$, respectively. Density studies of the alkali active sites were performed to elucidate the best activity for the catalyst composed with $SrFe_2O_4$.

Keywords: *Magnetic materials, strontium oxide, biodiesel, babassu oil.*

1. Introduction

The trend in the use of magnetic materials is constantly growing because of the ease of handling these materials. With a simple external magnetic field (magnet), they can be withdrawn from the reaction medium[1]. The most widely used magnetic materials in research and industries are the ferrites type[1–3].

The magnetite is the most common ferrites, it has the chemical formula $FeO.Fe_2O_3$ or Fe_3O_4, a spinel structure with an inverted cation distribution, where Fe^{+3} cations coordinate the oxygen ions in tetrahedral symmetry and the Fe^{+2} and Fe^{+3} occupy the octahedral sites in equivalent proportions[4,5]. However, other types of ferrites can be synthesized change the cation Fe^{+2} to other divalent metal, such as strontium, magnesium, barium, copper, nickel, cobalt and zinc[4].

The study of ferrites as solid support to catalysts is important, especially due an easy and quickly separation of the reaction medium. Moreover, they are ecologically correct, as they generate less discards to the environment[6]. They also can influence directly the catalytic effect of the material due to high surface area, robustness and alkalinity[7]. Moura *et al*[8,9] reported the effect of the use of cobalt ferrite ($CoFe_2O_4$) and magnesium ferrite ($MgFe_2O_4$) as support of Au^0 nanoparticles that were subsequently applied as catalysts in the oxidation reaction of benzyl alcohol.

Due to the constant study of heterogeneous catalysts for biodiesel production, the development of ferrites enriched with alkaline materials is relevant. However, few papers are published with these magnetic materials in transesterification reactions. Alves *et al*.[10] developed magnetic catalysts of Fe/Sn and Fe/Cd and used in the transesterification of soybean oil where they reached maximum yield of 86% after 1 hour of reaction at 200 °C. Falcão *et al*.[4] synthesized $SrO/CoFe_2O_4$ as a catalyst for transesterification reaction of babassu oil and obtained 96% yield under optimum conditions.

Our research group has been studying magnetic materials, with the proposal of using them as catalysts in oxidation of alcohols reactions, as well as in the transesterification of oils. Thus, in this study we performed the synthesis, characterization and use of Fe_3O_4 and $SrFe_2O_4$ enriched with strontium for the synthesis of biodiesel from babassu oil.

2. Experimental Procedures

2.1 Materials

All reagents were purchased from Sigma-Aldrich and used without further purification. $FeCl_2.4H_2O$ (98%), $FeCl_3.6H_2O$ (99%), $SrCl_2.6H_2O$ (99%), $SrCO_3$ (98%), acetone (99.9%), NH_4OH (28% NH_3 in water), methanol (99.9%), hydrochloric acid (37%), potassium hydrogen phthalate ($\geq$ 99.95%) and methyl heptadecanoate (99%) (internal stander). Refined babassu oil was purchased in local commerce (Teresina, Piauí, Brazil) and had an average molar mass of 725.05 g mol^{-1}, acid number equal to 0.8 mg NaOH g^{-1} and fatty acid composition described in Table 1.

*e-mail: mmoura@ufpi.edu.br

Table 1. Composition of fatty acids present in babassu oil.

Fatty acids	Value (%)
Caprylic acid (C8:0)	3.69 ± 0.42
Capric acid (C10:0)	4.13 ± 0.58
Lauric acid (C12:0)	45.10 ± 1.01
Myristic acid (C14:0)	16.28 ± 2.84
Palmitic acid (C16:0)	9.78 ± 1.01
Stearic acid (C18:0)	3.00 ± 1.55
Oleic acid (C18:1)	15.39 ± 0.27
Linoleic acid (C18:2)	2.63 ± 1.54

[a]Analysis made from the fatty acid methyl esters of babassu oil on a gas chromatography with flame ionization detector, equipped with a RTX-Wax capillary column and a temperature of 250 °C.

The composition of fatty acids present in babassu oil was carried out as follow: 100 mg of babassu oil was transferred to the centrifuge tube (20 mL), 2 mL of n-hexene (3 mL of the internal stander) and 0.2 mL of methanolic solution of KOH (2 mol L^{-1}). The tube was closed and shaken in a vortex for 30 seconds. After 3 mL of sodium chloride saturated solution was added.[11] The organic phase was separated and measure by gas chromatographic with FID detector.

2.2 Synthesis of SrO

The strontium oxide was obtained by the calcination of $SrCO_3$ at 1100 °C, for 5 hours in a muffle furnace of uncontrolled atmosphere[12]. After calcination the powder was kept in a desiccator for further uses.

2.3 Synthesis of Fe_3O_4 and $SrFe_2O_4$

The ferrites were prepared following the co-precipitation method proposed by Moura *et al.*[8] with some modification. An aqueous solution of $FeCl_3.6H_2O$ (5 mL, 8.2 mmol) and $FeCl_2.4H_2O$ (2.5 mL, 4.1 mmol) diluted in HCl (2 mol L^{-1}) were mixed. This mixture was dropped to 125 mL of aqueous NH_4OH solution (0.7 mol L^{-1}) and stirred for 30 minutes at room temperature. The precipitate obtained was collected with a magnet ($Nd_2Fe_{14}B$) and washed three times with distilled water and acetone. The solid (Fe_2O_4) was dried in an oven at 80 ° C for 12 hours.

The $SrFe_2O_4$ was prepared as follow: an aqueous solution of $FeCl_3.6H_2O$ (5 mL, 8.2 mmol) and $SrCl_2$ (2.5 mL, 4.1 mmol) were mixed. This mixture was dropped to 125 mL of aqueous NH_4OH solution (0.7 mol L^{-1}) and stirred for 2 hours at room temperature. The precipitate obtained was collected with a magnet ($Nd_2Fe_{14}B$) and washed three times with distilled water and acetone. The solid ($SrFe_2O_4$) was calcined in a muffle at 800 ºC for 3 hours.

2.4 Ferrites enrichment with SrO

The ferrite enrichment was performed according to the method proposed by Falcão *et al*[4]. Strontium oxide and Fe_3O_4 or $SrFe_2O_4$ were mixed in a molar proportion (5:1) in acetone.

The mixture stayed under stirring, at 65 °C for 24 hours. Afterward, the obtained solid was collected with a magnet ($Nd_2Fe_{14}B$) and dried in an oven at 80 °C for 12 hours.

2.5 Catalytic experiments

Transesterification reactions were performed using different experimental conditions. The modifications include the oil/alcohol molar ratio, amount of catalyst and reaction time. All experiments were carried out in a 250 mL flask connected to a condenser. The methyl alcohol and catalyst were stirred for 30 minutes and then the oil preheated at 65 °C[12,13] has been added. At the end of the reaction the catalyst has been magnetically separated, the excess of methanol has been removed in a rotary evaporator at 80 °C, and the glycerol has been separated from the product in the separatory funnel.

2.6 Characterizations

Fourier transform infrared spectroscopy (FTIR) analyzes have been performed on the PerkinElmer Spectrum 100 spectrometer, set to measure 16 cumulative scans at 4 cm^{-1} in a range between 4000 and 400 cm^{-1}. The samples have been prepared as KBr pellets (1:100 mg). The X-ray diffractograms (XRD) were obtained using a Bruker D8 Advance equipment, using monochromatic Cu Kα radiation ($\lambda = 1.54056$ Å) and graphite monochromator. The voltage of the copper emission tube was 40 kV and the filament current were 40 mA, the 2θ variation was from 10 to 90° with a 0.02° step size and a measurement time of 5 s/step. Identification of the phase composition presents in the catalysts were performed by Rietveld refinement using GSAS EXPGUI 2012 software. The magnetic characterizations were performed using an EZ9 MicroSense vibrating sample magnetometer (VSM) at room temperature with a magnetic field alternating between -1.7×10^3 and 1.7×10^3 kA/m. Thermogravimetric (TG) measurements were performed on a SHIMADZU DTG-60A equipment. The experiments were carried out in the temperature range of 30 to 1100 °C, using Pt crucible with approximately 10 mg sample, heating rate of 10 °C min^{-1} and nitrogen atmosphere (50 mL min^{-1}). The images used to determine the morphology and structure of the catalysts were observed in a scanning electron microscope (SEM) model SHIMADZU SSX-550 Superscan, where the samples were initially dispersed in isopropyl alcohol and fixed on carbon tape. The textural characteristics, such as Brunauer-Emmett-Teller (BET) specific area, pore volume and average pore diameter (Barrett-Joyner-Halenda, BJH) were determined by N_2 adsorption-desorption at 250 °C in an apparatus Quantachrome Novawin. The alkalinity of the catalysts was determined by volumetric analysis using a standard solution of 0.1 mol L^{-1} of potassium hydrogen phthalate (KHP), phenolphthalein as the indicator and calculated by dividing the number of moles KHP consumed by the mass of the catalyst used.

Magnetic Materials Enriched with Strontium: A Study of the use as Catalysts in the Transesterification
Reaction of Babassu Oil

3

The density of alkali active sites was determined from the values of alkalinity and surface area of the catalysts, using Equation 1[14].

$$\text{Density of alkali active sites} = \frac{\text{alkalinity}}{\text{catalyst area}} \quad (1)$$

The equipment used to analyze the fatty acid methyl esters (FAME) was a GC-FID 2010 of the Shimadzu, equipped with an RTX-Wax capillary column (0.32 mm x 30 m × 0.25 μm). Samples (1 μL) were applied with injector temperature and detector at 250 °C and column at 210 °C for 50 minutes. The entrainment gas was nitrogen (50 mL^{-1}). To prepare the samples, approximately 125 mg of biodiesel was weighed and dissolved in 2 mL of methyl heptadecanoate standard solution in chloroform (10 mg mL^{-1}). In the end, the FAME quantity has been determined according to Equation 2[14,15].

$$C_{FAME} = \frac{(\Sigma A) - A_{EI}}{A_{EI}} \times \frac{C_{EI} V_{EI}}{m} \times 100\% \quad (2)$$

Where C_{FAME} = quantity of fatty acid methyl esters; ΣA = total peak area of methyl esters comprising the range of C8:0 to C18:0; A_{EI} = area of methyl heptadecanoate (C17:0); C_{EI} = concentration of the C17:0 solution (mg mL^{-1}); V_{EI} = volume (mL) of the C17:0 solution added in the sample; m = weight (mg) of the sample.

3. Results and Discussion

3.1 Catalysts characterization

The use of magnetic supports in the synthesis of heterogeneous catalysts provides fast, efficient and ecological separation[6,9]. In this study, as previously reported, the co-precipitation method has been used to prepare the ferrites under alkaline conditions, which makes the procedure simple and result a satisfactory magnetic properties material.

The magnetic force of the catalysts has been analyzed through the applied magnetic field, varying from +1.7.10^3 to -1.7.10^3 kA/m obtaining hysteresis loops characteristic of the materials (Figure 1).
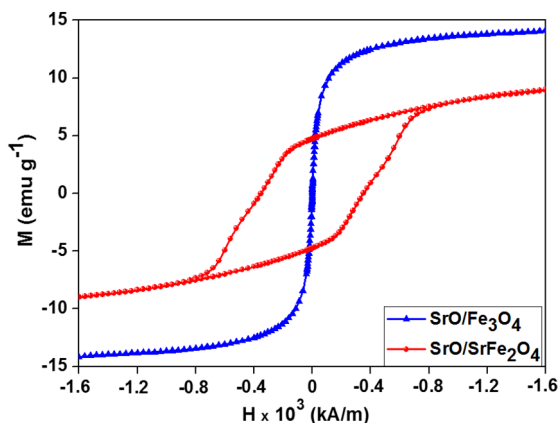

Figure 1. Magnetization as a function of the applied magnetic field for bare SrO/Fe$_3$O$_4$ and SrO/SrFe$_2$O$_4$ at room temperature.

The magnetization results of the SrO/Fe$_3$O$_4$ catalyst indicated the formation of a ferromagnetic compound. No coercive field or hysteresis at room temperature. This allows for instant separation using a magnet (Nd$_2$Fe$_{14}$B) and immediate redispersion when the magnet is removed. The catalyst SrO/SrFe$_2$O$_4$ showed a formation of hysteresis at room temperature, however a decrease the magnetic force has been observed. Nevertheless, both catalysts have magnetic properties acceptable for the proposal of this work.

The composition of the catalysts has been analyzed by X-ray diffractometry (XRD) followed by Rietveld refinement. Figure 2a shows the diffractogram of SrO/Fe$_3$O$_4$, and it can be seen four 4 crystalline phases: Fe$_3$O$_4$ (ICSD 84611), SrO (ICSD 26960), SrCO$_3$ (ICSD 202793) and Sr(OH)$_2$.H$_2$O (ICSD 15366). The refined data showed 15% of magnetite 30% of SrO, SrCO$_3$ (5%) and Sr(OH)$_2$.H$_2$O (50%).
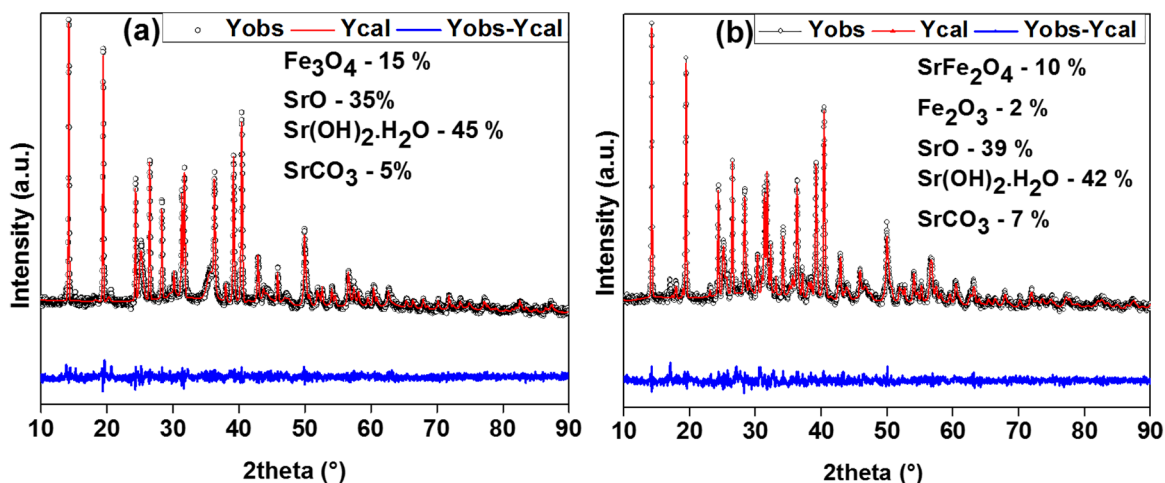

Figure 2. Rietveld refinement plot for (a) SrO/Fe$_3$O$_4$ and (b) SrO/SrFe$_2$O$_4$ catalysts, showing the observed, calculated and difference pattern.

The strontium hydroxide, according to the literature is associated with the decomposition mechanism of the precursor (SrO), where the carbonate and water vapor present in the atmosphere react forming hydroxide and CO_2[12,14,16]. The strontium hydroxide, in accordance to our previous works, does not have catalytic activity in the transesterification reaction[12,14].

The crystalline phases found to $SrO/SrFe_2O_4$ (Figure 2b) were: $SrFe_2O_4$ (ICSD 66403), Fe_2O_3 (ICSD 82134), SrO (ICSD 26960), $SrCO_3$ (ICSD 202793) and $Sr(OH)_2.H_2O$ (ICSD 15366). The presence of $SrFe_2O_4$ (10%) demonstrates the efficiency in the synthesis process of the compound, where the Fe^{+2} ions were replaced by Sr^{+2} ions, being that only 2% of the ferrite (Fe_2O_3) was not exchanged. The SrO/$SrFe_2O_4$ catalyst also showed SrO (39%), $SrCO_3$ (7%) and $Sr(OH)_2.H_2O$ (42%).

To corroborate the XRD results, the catalysts were further analyzed by FTIR and TG. The TG/DTGA curves (Figure 3a, 3b) showed three weight loss of similar and specific masses. The first event occurs between 100 and 140 °C and is related to the evaporation of water adsorbed on the surface of materials[12], the second one range to 450-580 °C was associated to the decomposition of strontium hydroxide[17].

The third event has been occurred at temperature above 750 °C and refers to the decomposition of $SrCO_3$ residual[18]. The thermogravimetric measurements showed that the synthesized ferrites presented good thermal stability since no event characteristic of the decomposition of these materials has been observed.

The FTIR results of the SrO/Fe_3O_4 and $SrO/SrFe_2O_4$ catalysts showed stretching bands in the region of 3488 and 3600 cm^{-1} attributed to the O-H bond of the strontium hydroxide molecule[19]. Bands at 3000 - 3200 cm^{-1} have been attributed to hydroxyls groups present in water adsorbed[17]. The stretching and deformation bands of strontium carbonate has been observed at 1460 and 862 cm^{-1}, respectively[12,17]. The stretching band of Sr-O was observed at 596 cm^{-1}.[12] The stretching bands at 600 cm^{-1} and 598 cm^{-1} have been attributed to the Fe-O of the Fe_3O_4 and $SrFe_2O_4$, and a band at 459 cm^{-1} was relative to Sr-O binding of $SrFe_2O_4$[19,20].

The structural and morphological characterization of the SrO/Fe_3O_4 and $SrO/SrFe_2O_4$ catalysts is shown in Figure 4. The SEM images showed irregular particle agglomerates of different sizes. These groupings promote a decrease in the surface area, but with tendencies of improvement contact of the substrate and catalyst[14].
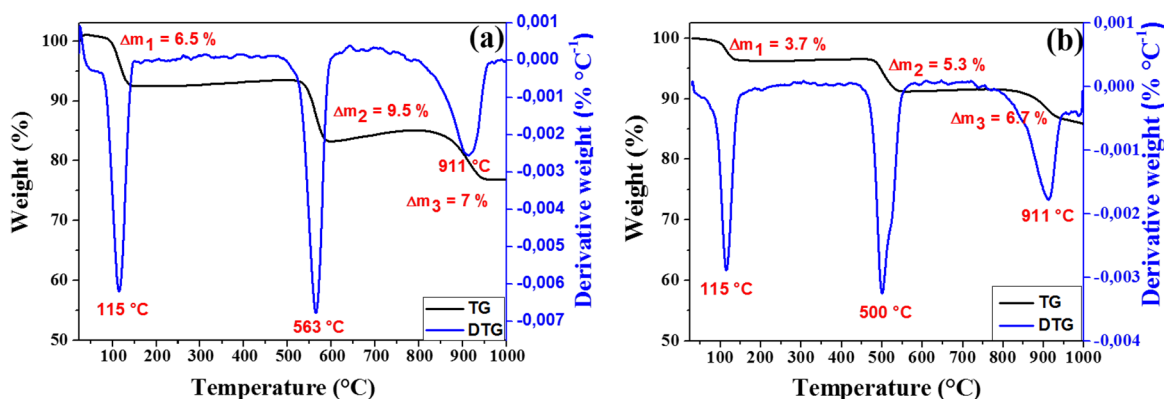

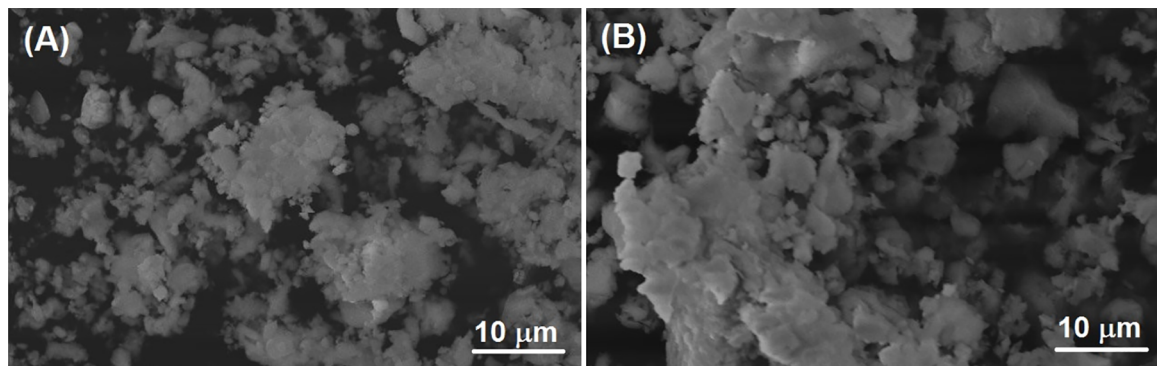**Figure 3.** TG/DTG curves of the (a) SrO/Fe_3O_4 and (b) $SrO/SrFe_2O_4$ catalysts.

Figure 4. SEM images of the (a) SrO/Fe_3O_4 and (b) $SrO/SrFe_2O_4$ catalysts.

Magnetic Materials Enriched with Strontium: A Study of the use as Catalysts in the Transesterification
Reaction of Babassu Oil

5

Surface area studies (Figure 5) showed adsorption and desorption isotherms not completely reversible, i.e, the curves are not overlapping, being characteristic of a type IV isotherm of the BET (Brunauer-Emmett-Teller) system[21]. The type of hysteresis that occurs in the adsorption process is called capillary condensation, which indicates the formation of mesoporous material[21,22]. The results of specific surface area (ASS_{BET}), average pore diameter (d_{pores}), average pore volume (V_{pores}), alkalinity and density of alkaline sites are listed in Table 2. An increase of ASS_{BET}, d_{pores}, and V_{pores} has been observed, when compared with the catalysts described by our research group and the literature. The difference may be related the strontium oxide is supported on the magnetic material[4,12,13,17,23].

The density of alkaline sites was also studied for further understanding of the potential of materials as catalysts in the synthesis of methyl esters. According to Semwal *et al.*[24]

and Marwaha *et al.*[25], the synthesis of biodiesel using heterogeneous alkaline catalysts can lead to a greater conversion to FAME, as well as a reduction of production costs when compared with heterogeneous acid catalysts.

$SrO/SrFe_2O_4$ presented higher alkaline force when compared to SrO/Fe_3O_4, which is possibly related to higher strontium quantity.

3.2 Catalytic experiments

Conversion to FAME can be affected by catalyst type, oil/alcohol molar ratio, temperature and time.[26,27] In this study, experiments were carried out to optimize the best reaction conditions in order to achieve the highest conversion to esters.

The amount of the catalyst (related to the mass of oil) was investigated using 1:6 oil/alcohol molar ratio, at 65 °C for 4 hours. The results (Figure 6a) showed that the SrO/Fe_3O_4 catalyst presented better activity, when 6% was used.
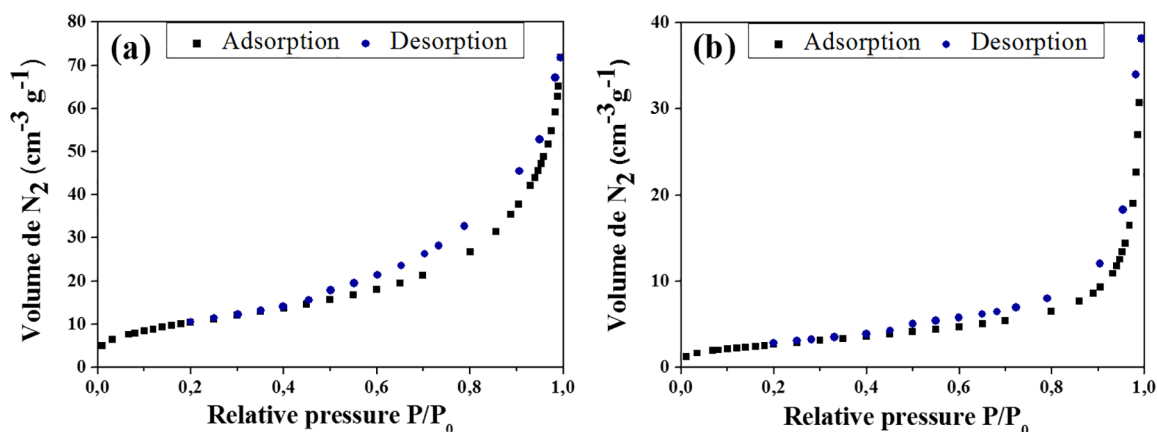

Figure 5. Nitrogen adsorption-desorption isotherms of the (a) SrO/Fe_3O_4 and (b) $SrO/SrFe_2O_4$ catalysts.
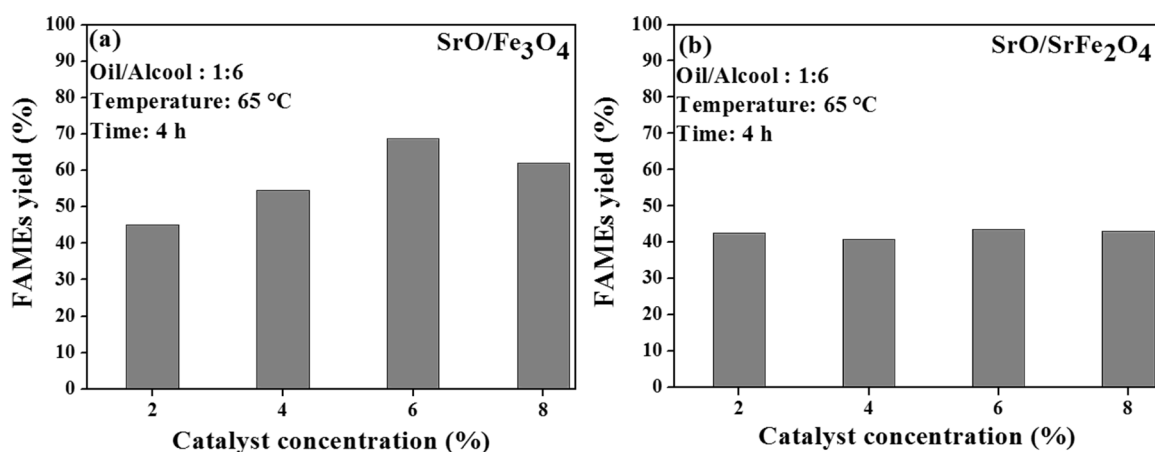

Figure 6. Effect of the concentration of the (a) SrO/Fe_3O_4 and (b) $SrO/SrFe_2O_4$ catalysts in relation to the babassu oil for the production of biodiesel.

Table 2. Results of nitrogen adsorption analysis.

Catalyst	ASS_{BET} (m² g⁻¹)	d_{pores} (Å)	V_{pores} (cm³ g⁻¹)	Alkalinity (mol g⁻¹)	Density of alkaline sites (mol m²)
SrO/Fe_3O_4	38.67 ± 0.14	105.90	0.105	5.44.10-6 ± 0.039	1.40.10-9 ± 0.07
$SrO/SrFe_2O_4$	12.31 ± 0.06	185.709	0.059	5.44.10-6 ± 0.040	4.42.10-9 ± 0.12

ASS_{BET}: specific surface area; d_{pores}: average pore diameter; V_{pores}: average pore volume.

The larger quantity causes a decrease in FAME content, and this is a consequence of the alcohol decrease, catalyst and oil diffusion[14]. The amount of SrO/SrFe$_2$O$_4$ catalyst (Figure 6b) was varied from 2 to 8%, and the conversion of the oil to ester was practically the same. Then the amount of 2% of the catalyst was chosen for the other optimizations.

The effect of the oil/alcohol molar ratio has been studied using time and temperature conditions equal to 4 hours and 65 °C. The concentrations of the catalysts were applied according to the previous study, 6% for SrO/Fe$_3$O$_4$ and 2% for SrO/SrFe$_2$O$_4$. Figure 7 shows the conversion of the fatty acids methyl ester (FAME) obtained during the optimization of the oil and alcohol ratio.

Stoichiometrically the oil/alcohol molar ratio required for the transesterification reaction is 1:3, however, this ratio is not sufficient to complete the reaction, due to the reversibility of the transesterification, thus a higher molar ratio is required[28]. The results shown in Figure 7, for both catalysts, confirm that the oil and alcohol molar ratio of 1:

3 was not enough for good conversion to esters. However, with the molar ratio 1:9 for the SrO/Fe$_3$O$_4$ catalyst and 1:15 for the SrO/SrFe$_2$O$_4$ catalyst was obtained the best FAME conversion.

The time parameter was optimized using 65 ºC, 6% of SrO/Fe$_3$O$_4$ and 2% of SrO/SrFe$_2$O$_4$ catalysts, and the 1:9 and 1:15 oil/alcohol molar ratio, for the respective catalysts. Figure 8 shows the relationship between the reaction times and the FAMEs conversion obtained.

The best results were achieved at the reaction time of 4 hours for both catalysts. Conversions in FAME were 78.6% and 89.7% for the SrO/Fe$_3$O$_4$ and SrO/SrFe$_2$O$_4$ catalysts, respectively. Higher reaction times reduced conversion to esters. This decrease is due to the reversibility of the reaction which leads to the formation of salts of residual fatty acids[29].

The SrO/SrFe$_2$O$_4$ catalyst showed the best results in the conversion in FAME. This fact is related to a greater amount of alkaline active sites compared to the SrO/Fe$_3$O$_4$ catalyst.
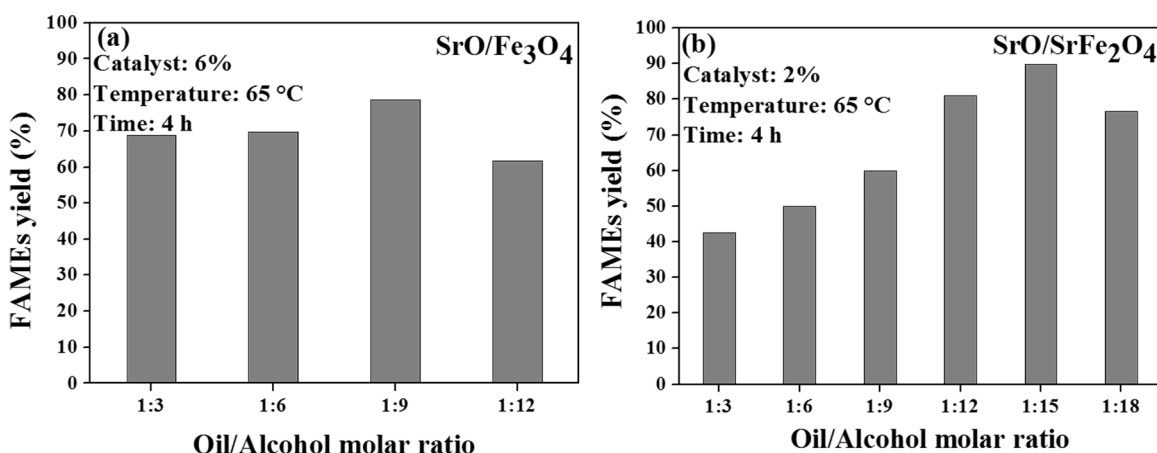

Figure 7. Effect of the oil/alcohol molar ratio on the transesterification reaction of babassu oil for biodiesel production, using (a) SrO/Fe$_3$O$_4$ and (b) SrO/SrFe$_2$O$_4$ catalysts.
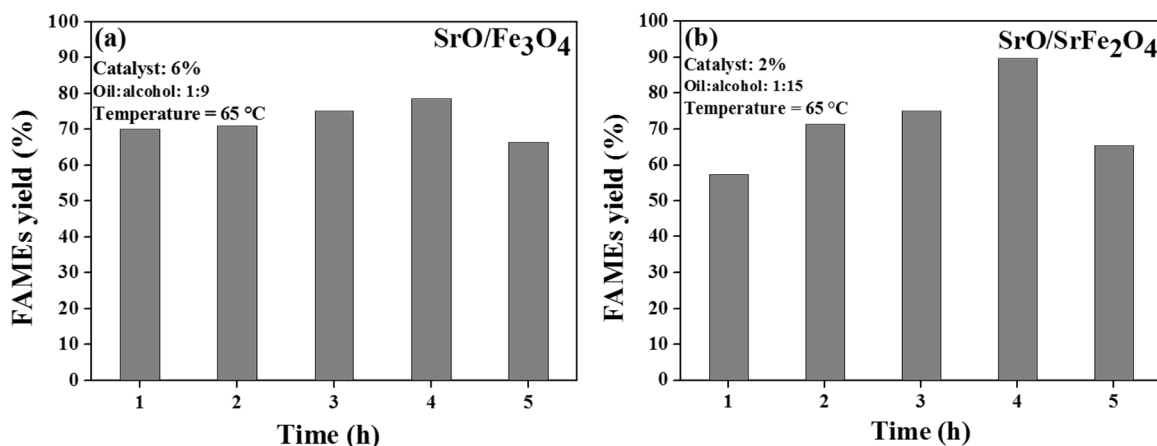

Figure 8. Effect of reaction time on the transesterification reaction of babassu oil for biodiesel production, using (a) SrO/Fe$_3$O$_4$ and (b) SrO/SrFe$_2$O$_4$ catalysts.

Magnetic Materials Enriched with Strontium: A Study of the use as Catalysts in the Transesterification Reaction of Babassu Oil

7

4. Conclusions

The analyzes performed in this study show that the ferrites synthesized by the easy co-precipitation method were successfully obtained. We also observed that hydroxide and carbonate strontium are present in the structure of strontium oxide. The VSM analysis showed that both catalysts have satisfactory magnetic characteristics for the proposal. The catalytic experiments presented higher biodiesel yield (78.6%) for the SrO/Fe_3O_4 catalyst when 6% of catalyst, 1:9 oil/alcohol molar ratio, 4 hours and 65 ° C were used. When the $SrO/Sr_2Fe_2O_4$ was applied under conditions of 2% catalyst concentration, oil/alcohol molar ratio of 1:15, reaction time and temperature of 4 and 65 °C, the highest biodiesel conversion was obtained in this study (89.7%). Studies the alkaline active sites of the catalysts proposed a higher reaction favoritism to material $SrO/SrFe_2O_4$ when compared to SrO/Fe_3O_4 during transesterification.

5. Acknowledgments

6. References

1. Kaneyoshi T. Compensation temperature in a cylindrical Ising nanowire (or nanotube). *Physica A: Statistical Mechanics and its Applications*. 2011;390(21-22):3697-3703.

2. Mert G. Green's function study of a three-sublattice mixed-spin Heisenberg ferromagnetic and ferrimagnetic system. *Journal of Magnetism and Magnetic Materials*. 2014;363:224-231.

3. Al-Omari A. Thermal Properties of Ferrimagnetic Systems. *World Journal of Condensed Matter Physics*. 2011;1(4):121-129.

4. Falcão MS, Garcia MAS, De Moura CVR, Nicolodi S, de Moura EM. Synthesis, Characterization and Catalytic Evaluation of Magnetically Recoverable $SrO/CoFe_2O_4$ Nanocatalyst for Biodiesel Production from Babassu Oil Transesterification. *Journal of the Brazilian Chemical Society*. 2018;29(4):845-855.

5. Pereira G, Martins A. Educação. *Quim Nova* 2008; 31: 430–432.

6. Rossi LM, Costa NJS, Silva FP, Wojcieszak R. Magnetic nanomaterials in catalysis: advanced catalysts for magnetic separation and beyond. *Green Chemistry*. 2014;16(6):2906-2933.

7. Mokhtary M, Torabi M. Nano magnetite (Fe_3O_4), an efficient and robust catalyst for the one-pot synthesis of 1-(aryl(piperidin-1-yl)methyl)naphthalene-2-ol and 1-(α-amido alkyl)-2-naphthol under ultrasound irradiation. *Journal of Saudi Chemical Society*. 2017;21(Suppl 1):S299-S304.

8. de Moura EM, Garcia MAS, Gonçalves RV, Kiyohara PK, Jardim RF, Rossi LM. Gold nanoparticles supported on magnesium ferrite and magnesium oxide for the selective oxidation of benzyl alcohol. *RSC Advances*. 2015;5(20):15035-15041.

9. de Abreu WC, Garcia MAS, Nicolodi S, de Moura CVR, de Moura EM. Magnesium surface enrichment of $CoFe_2O_4$ magnetic nanoparticles immobilized with gold: reusable catalysts for green oxidation of benzyl alcohol. *RSC Advances*. 2018;8(7):3903-3909.

10. Alves MB, Medeiros FCM, Sousa MH, Rubim JC, Suarez PAZ. Cadmium and Tin Magnetic Nanocatalysts Useful for Biodiesel Production. *Journal of the Brazilian Chemical Society*. 2014;25(12):2304-2313.

11. Hartman L, Lago RC. Rapid preparation of fatty acid methyl esters from lipids. *Laboratory Practice*. 1973;22(6):475-476.

12. de Carvalho LMG, de Abreu WC, Silva MGO, Lima JRO, de Oliveira JE, de Matos JME, et al. Heterogeneous catalysis afford biodiesel of babassu, castor oil and blends. *Journal of the Brazilian Chemical Society*. 2013;24(4):550-557.

13. Liu X, He H, Wang Y, Zhu S. Transesterification of soybean oil to biodiesel using SrO as a solid base catalyst. *Catalysis Communications*. 2007;8(7):1107-1111.

14. de Abreu WC, de Moura CVR, Costa JCS, de Moura EM. Strontium and Nickel Heterogeneous Catalysts for Biodiesel Production from Macaw Oil. *Journal of the Brazilian Chemical Society*. 2017;28(2):319-327.

15. Thoai DN, Photaworn S, Kumar A, Prasertsit K, Tongurai C. A Novel Chemical Method for Determining Ester Content in Biodiesel. *Energy Procedia*. 2017;138:536-543.

16. L'vov BV. Mechanism of thermal decomposition of alkaline-earth carbonates. *Thermochimica Acta*. 1997;303(2):161-170.

17. Granados-Correa F, Bonifacio-Martínez J. Combustion synthesis process for the rapid preparation of high-purity SrO powders. *Materials Science-Poland*. 2014;32(4):682-687.

18. Bacce ED, Pires AM, Davalos MR, Jafelicci M Jr. Thermal decomposition and rehydration of strontium oxalate: morphological evolution. *International Journal of Inorganic Materials*. 2001;3(6):443-452.

19. Javidan A, Rafizadeh S, Hosseinpour-Mashkani SM. Strontium ferrite nanoparticle study: Thermal decomposition synthesis, characterization, and optical and magnetic properties. *Materials Science in Semiconductor Processing*. 2014;27:468-473.

20. Soares PIP, Machado D, Laia C, Pereira LCJ, Coutinho JT, Ferreira IMM, et al. Thermal and magnetic properties of chitosan-iron oxide nanoparticles. *Carbohydrate Polymers*. 2016;149:382-390.

21. Brunauer S, Deming LS, Deming WE, Teller E. On a Theory of the van der Waals Adsorption of Gases. *Journal of the American Chemical Society*. 1940;62(7):1723-1732.

22. Schneider P. Adsorption isotherms of microporous-mesoporous solids revisited. *Applied Catalysis A: General*. 1995;129(2):157-165.

23. Dias APS, Bernardo J, Felizardo P, Correia MJN. Biodiesel production by soybean oil methanolysis over SrO/MgO catalysts: The relevance of the catalyst granulometry. *Fuel Processing Technology*. 2012;102:146-155.

24. Semwal S, Arora AK, Badoni RP, Tuli DK. Biodiesel production using heterogeneous catalysts. *Bioresource Technology*. 2011;102(3):2151-2161.

25. Marwaha A, Dhir A, Mahla SK, Mohapatra SK. An overview of solid base heterogeneous catalysts for biodiesel production. *Catalysis Reviews: Science and Engineering*. 2018;60(4):594-628.

26. Ramadhas AS, Jayaraj S, Muraleedharan C. Biodiesel production from high FFA rubber seed oil. *Fuel*. 2005;84(4):335-340.

27. Koh MY, Ghazi TIM. A review of biodiesel production from *Jatropha curcas L*. oil. *Renewable and Sustainable Energy Reviews*. 2011;15(5):2240-2251.

28. Yu X, Wen Z, Li H, Tu ST, Yan J. Transesterification of *Pistacia chinensis* oil for biodiesel catalyzed by CaO-CeO$_2$ mixed oxides. *Fuel*. 2011;90(5):1868-1874.

29. Leung DYC, Guo Y. Transesterification of neat and used frying oil: Optimization for biodiesel production. *Fuel Processing Technology*. 2006;87(10):883-890.